Title
Modeling the Impact of Land Surface Degradation on the Climate of Tropical North Africa

Journal
Journal of Climate, 14(8)

ISSN
0894-8755

Authors
Clark, Douglas B
Xue, Yongkang
Harding, Richard J
et al.

Publication Date
2001-04-01

DOI
10.1175/1520-0442(2001)014<1809:mtiols>2.0.co;2

Peer reviewed

Modeling the Impact of Land Surface Degradation on the Climate of Tropical North Africa

DOUGLAS B. CLARK

Centre for Ecology and Hydrology, Wallingford, Oxfordshire, United Kingdom

YONGKANG XUE

Department of Geography, University of California, Los Angeles, Los Angeles, California

RICHARD J. HARDING

Centre for Ecology and Hydrology, Wallingford, Oxfordshire, United Kingdom

PAUL J. VALDES

Department of Meteorology, University of Reading, Reading, United Kingdom

(Manuscript received 25 February 2000, in final form 1 August 2000)

ABSTRACT

Degradation of the land surface has been suggested as a cause of persistent drought in tropical north Africa. A general circulation model is used to assess the impact of degradation of five regions within tropical north Africa. Idealized degradation scenarios are used since existing observations are inadequate to determine the extent and severity of historical degradation. It is found that the impact of degradation varies between the regions. The greatest effects are found from degradation of the Sahel or West Africa, which result in substantial reduction of precipitation over the degraded area. Both surface evaporation and atmospheric moisture convergence are reduced. In the Sahelian case the precipitation reduction extends well to the south of the area of changed land surface. The occurrence of easterly wave disturbances is not altered by degradation, but the mean rainfall from each event is reduced. Degradation of an area in eastern north Africa results in smaller reductions of precipitation and moisture convergence. Finally, degradation of a southern area next to the Gulf of Guinea has little effect on precipitation because of a compensatory increase of moisture convergence. The simulated rainfall reduction following degradation of the Sahel is comparable to observed changes in recent decades, suggesting that degradation may have contributed to that change.

1. Introduction

Rainfall has a profound effect on the lives of millions of people in tropical north Africa (TNA) through its effects on the availability of water for agriculture and domestic use. (In this study TNA is defined as that part of Africa between the equator and the Sahara.) Several studies have documented the variability of rainfall in TNA on interannual and longer timescales (e.g., Hulme 1992a; Lamb and Peppler 1991; Nicholson 1993; Nicholson and Palao 1993; Rowell et al. 1995). The 1950s were relatively wet in the Sahel, but by the end of the 1960s the area was experiencing relatively dry conditions that persisted for much of the next 30 years, with the 1980s being the driest decade of the century (Nicholson 1993). Figure 1 shows the observed difference in rainfall over TNA between the periods 1931–60 and 1961–90. The data come from an updated version of the gridded, gauge-based climatology described by Hulme (1992b). In the later period there was less precipitation in a band across the continent north of approximately 10°N, but increased rainfall in the Guinea coast and Cameroon areas. Such anticorrelation of interdecadal rainfall anomalies in the Sahel and Guinea coast has been noted in previous studies (e.g., Hulme 1992a; Nicholson and Palao 1993; Rowell et al. 1995), although recent decades have seen a shift to positive correlation (Nicholson 1993; Janicot et al. 1996). The deficit in the Sahel[1] seen in Fig. 1 was equivalent to 19% of the mean

Corresponding author address: Dr. Douglas B. Clark, Centre for Ecology and Hydrology, Wallingford, Oxfordshire OX10 8BB, United Kingdom.
E-mail: dbcl@ceh.ac.uk

[1] Subdivisions of TNA used in this work are closely based on those of Rowell et al. (1995): the Sahel 12.5°–17.5°N, 15°W–37.5°E, and the Guinea coast 5°–10°N, 7.5°W–7.5°E.

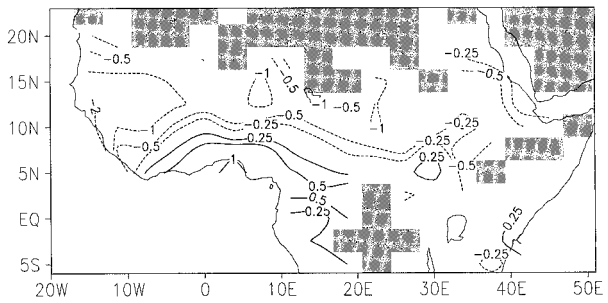

FIG. 1. Observed difference in JAS mean precipitation rate (mm day^{-1}) between the periods 1931–60 and 1961–90, using the rainfall climatology of Hulme (1992b). The plotted field is the difference (1961–90) − (1931–60). Isohyets are drawn at ±0.25, 0.5, 1, and 2 mm day^{-1}. Land points without data are shaded.

for 1931–60 and was at least partly responsible for great human suffering in the area that attracted international attention.

This persistently low rainfall may have been caused by anthropogenic modification of the land surface. Charney (1975) used a dry linear model to show that increasing the land surface albedo in TNA north of 18°N resulted in increased radiative cooling of the atmosphere and compensating descent, which would tend to suppress rainfall. Charney et al. (1977) increased the albedo of the Sahel in runs of a general circulation model (GCM) that also included moist processes, and these did indeed show reduced rainfall. It was argued that less radiation absorbed by the surface meant a smaller flux of moist static energy (H + LE, where H and LE are the sensible and latent heat fluxes, respectively) into the atmosphere, which tended to reduce moist convection. Since then there have been several GCM studies showing an effect of the land surface on tropical precipitation (e.g., Polcher 1995; Lean and Rowntree 1997). Many of these studies have shown that a dry surface and/or high albedo following degradation result in less rainfall over the tropical continents. Supporting evidence is provided by studies based on one-dimensional models that have indicated that moist convection is greater over a moist and/or vegetated surface (Clark and Arritt 1995; Segal et al. 1995; De Ridder 1997). The difficulty of interpreting complex GCM experiments has led some to consider degradation in simpler models. In particular, Zheng and Eltahir (1998) used the theory of steady-state, axisymmetric flows to argue that the impact of deforestation was to reduce the entropy in the boundary layer, thereby lessening the meridional gradient of entropy between ocean and land, and weakening the meridional circulation.

The particular question of land degradation in TNA has been investigated by Xue and Shukla (1993) and Xue (1997). Both these studies used the GCM of the Center for Ocean–Land–Atmosphere Studies (COLA) to investigate the impact of degradation of 9°–18°N across TNA. Xue and Shukla (1993) formed ensembles of 3-month integrations and found that June–August rainfall over the degraded area was reduced by 1.5 mm day^{-1} (22%), while it was increased over the Guinea coast in a pattern reminiscent of observed changes. Since reduced rainfall was confined to the degraded area, the specification of which was somewhat arbitrary, it was recommended that future work should investigate the sensitivity to degradation of different areas. Xue (1997) degraded the same area, but used multiyear runs and again found that Sahelian rainfall was substantially reduced in the wet season. The present work builds on these studies by using the COLA GCM to examine the impact of degradation of smaller areas of TNA than were examined by Xue and Shukla (1993) and Xue (1997).

Alternatively it may be that variation of global sea surface temperature (SST) has caused the reduced rainfall in TNA. Rowell et al. (1995) showed that observed global SST and rainfall in TNA were correlated, and a physical basis for these empirical results was suggested by the skill shown by GCM integrations using observed SST for 10 chosen years. However, the strength of the correlation may be lower in other years (Sud and Lau 1996). It may well be that SST and land surface effects interact and need to be considered simultaneously. Global SST may set the large-scale conditions that are then modulated by local land surface conditions (Lare and Nicholson 1994; Diedhou and Mahfouf 1996). SST might favor a relatively wet year in the Sahel but, if land surface degradation affected the initiation or longevity of rainfall systems, the result could be less rainfall than would have occurred had the surface not been degraded. Rowell et al. (1995) and Diedhou and Mahfouf (1996) investigated the relative strengths of land surface and SST effects in idealized cases, but this is an issue that should benefit from further modeling work. To simplify the analysis, the effects of SST are not considered further in the present work.

In this work ''land surface degradation'' is taken to be synonymous with ''desertification'' and to result mainly from adverse human impact, following the definition adopted by the United Nations Environment Program (UNEP) in 1991 (see Dregne et al. 1991). In recent years there has been considerable debate as to what desertification really is and how much, if any, has occurred in TNA, with a review in the meteorological literature provided by Nicholson et al. (1998). For the present purpose, degradation is considered to result in long-term reduction of the vegetation cover. This is quite different from interannual variability of vegetation in response to rainfall that is described by Tucker et al. (1991). The difficulty of separating this signal from that of long-term changes is one reason why the extent of degradation is difficult to determine.

UNEP (1992) estimated that almost 28% of the area defined as the Sahel suffered from soil degradation (vegetation was not considered). However, Nicholson et al. (1998) concluded that widespread changes of vegetation cover and productivity had not occurred in the drought

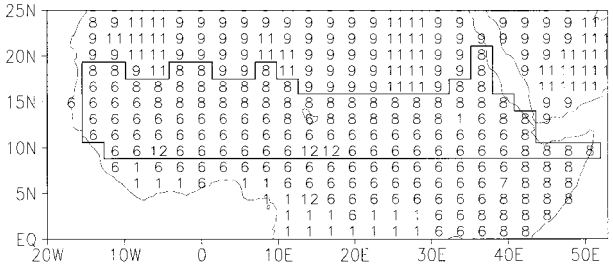

FIG. 2. The distribution of biome types in tropical north Africa for the control integrations. The area outlined was degraded by Xue and Shukla (1993) and Xue (1997). Biome types are 1 broadleaf evergreen trees, 6 broadleaf trees with groundcover, 7 groundcover only, 8 broadleaf shrubs with perennial groundcover, 9 broadleaf shrubs with bare soil, 11 bare soil, and 12 crops.

years of the 1980s and the early 1990s. Thus, although there may have been some land surface degradation in recent decades, the extent and severity of this are extremely difficult to determine. It may be that the existing data are insufficient to assess the extent of historical degradation. However, the human population of West Africa is rapidly increasing, so that by 2050 the population is expected to be over three times as large as in 1995 (Fischer and Heilig 1997). Pressure on the land is likely to increase accordingly and the question of the potential of degradation to alter climate remains of key interest.

The remainder of this paper is arranged as follows. First, the GCM and its simulation of the control climate are discussed in section 2, then the next section describes the degradation scenarios used. The impact on seasonal mean rainfall is presented in section 4, while section 5 discusses the results of one scenario in some detail. An intercomparison of the results from different scenarios is given in section 6, followed by a discussion of the results.

2. The numerical model and control integrations

a. The COLA GCM

The COLA GCM is a global spectral model, described by Kinter et al. (1988) and Fennessy et al. (1994). The version used had R40 truncation with a Gaussian grid of 128 × 102 points, giving a grid box size at the equator of 2.8° longitude × 1.8° latitude. A normalized pressure (σ) coordinate was used in the vertical, with 18 equally spaced levels, and mean orography is used. The subgrid-scale vertical transfer of heat, moisture, and momentum were parameterized by the level 2.0 second-order scheme of Mellor and Yamada (1982). Radiative transfer was calculated following Harshvardhan et al. (1987). Clouds were described using a diagnostic cloud scheme following Slingo (1987), with interaction with radiation as implemented by Hou (1990). Penetrative convection was parameterized after Kuo (1965), as modified by Anthes (1977), while shallow convection followed Tiedtke (1983).

Turbulent fluxes in the lowest layer were calculated using Monin–Obukhov similarity theory. Fluxes over land were calculated using the Simplified Simple Biosphere model (SSiB) of Xue et al. (1991). SSiB represents the total evaporation as the sum of transpiration, evaporation of water stored on the canopy, and bare soil evaporation, while a three-layer soil water model calculates fluxes according to Darcy's law. At each land point the combination of vegetation and soil is specified as being 1 of 12 biome types, the global distribution of which is based on Kulcher (1984). Figure 2 shows the distribution of biome types over TNA in the control ensemble. The biomes were described by Xue et al. (1991) as 1 broadleaf evergreen trees, 6 broadleaf trees with groundcover, 7 groundcover only, 8 broadleaf shrubs with perennial groundcover, 9 broadleaf shrubs with bare soil, 11 bare soil, and 12 crops. Selected characteristics of the main biomes found in TNA are listed in Table 1.

Climatological monthly mean SST (Bottomley et al. 1990) for the period 1951–80 was used in all integrations. The effect of degradation of any region was considered as the difference between a degradation ensemble for which the land surface was altered as described in section 3 below, and a control ensemble in which the land surface characteristics represented the undegraded

TABLE 1. Values of selected parameters for SSiB biomes found in tropical north Africa. Values are shown for biome types 1 (broadleaf evergreen trees), 6 (trees with groundcover), 8 (shrubs with groundcover), and 9 (shrubs with bare soil).

	Type 1	Type 6	Type 8	Type 9
Surface albedo[a,b]	0.13	0.20	0.20	0.30
Roughness length (m)[a]	2.65	0.95	0.25	0.06
Vegetated fraction	0.98	0.30	0.10	0.10
Leaf area index[a,c]	5.0	4.1	0.9	0.3
Minimum stomatal resistance (s m^{-1})	153	165	855	855
Root depth (m)	1.0	0.5	0.5	0.5
Volumetric moisture at wilting point	0.12	0.13	0.05	0.04
Volumetric moisture at saturation	0.42	0.42	0.44	0.44
Hydraulic conductivity at saturation × 10^5 (m s^{-1})	2.0	2.0	17.6	17.6
Matric potential at saturation (m)	−0.086	−0.086	−0.035	−0.035

[a] JAS mean value for a parameter with monthly variation.
[b] Surface albedo was as calculated in the control ensemble.
[c] Canopy capacity (mm) is given by 0.1 × leaf area index.

state. Each ensemble consisted of four members that differed only in the initial atmospheric condition. The initial conditions were analyses for 1 June 1987 and 1, 2, 3 June 1988, and all integrations were for four months. Analysis was concentrated on July–August–September (JAS) since this is the important season across much of TNA, particularly in the Sahel where up to 90% of the annual total falls in these months (Rowell et al. 1995).

Soil moisture was initialized using the procedure described by Sato et al. (1989) to transform the climatology of Mintz and Walker (1993) into a form suitable for SSiB. Given that each GCM integration was only 4 months long, the initial soil moisture may have had considerable influence on the results. The large fraction of bare soil prescribed for much of the vegetation (Table 1) meant that the bare soil component was a large part of the total evaporation across much of TNA. Since this is maintained by moisture in a thin top layer of soil that is frequently wetted by precipitation, the impact of the initial soil moisture field was lessened. Ultimately the extent to which the initial condition and possible spinup affected the short integrations used here can only be analyzed by comparison with longer integrations. Xue (1997) performed multiyear integrations of the same GCM and reported that for many variables, including evaporation and precipitation, the long-term spinup of hydrology was relatively unimportant, so computationally cheaper seasonal integrations were useful.

b. Comparison of control integration with observations

The control ensemble was verified against a variety of observational and reanalysis data. The main results are summarized here, while further details are given by Clark (1999). Figure 3 shows the modeled JAS mean precipitation rate and its difference from the mean for 1931–60 from Hulme's climatology. The climatology was regridded onto the GCM grid for this comparison. The simulated precipitation shown in Fig. 3a captured much of the basic structure observed, with the maximum rainfall near 9°N on the west coast. However, Fig. 3b shows that there was less rainfall than observed in both the Sahel and equatorial regions. The largest discrepancies were in the area of Ethiopia where the modeled precipitation was greatly in excess. It is particularly difficult to determine a representative rainfall in such a mountainous area and some grid boxes were represented by only one station in Hulme's data. However, there were consistent errors relative to other reference periods and other rainfall climatologies, also relative to observed cloud cover (from the International Satellite Cloud Climatology Project; Schiffer and Rossow 1983) and outgoing longwave radiation (Earth Radiation Budget Experiment; Barkstrom 1984), which suggested that the simulation was indeed poor in this area. Across TNA there was insufficient seasonality in the simulated precipitation.

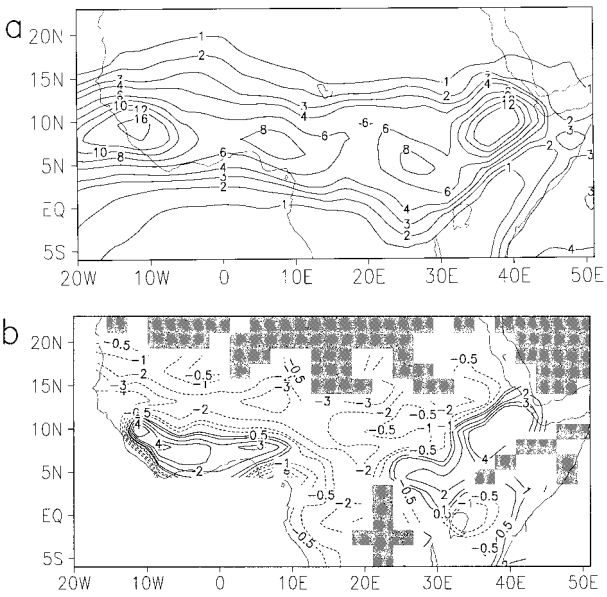

FIG. 3. JAS mean precipitation rate (mm day^{-1}). (a) Control ensemble mean. Isohyets are drawn at 1, 2, 3, 4, then every 2 mm day^{-1}. (b) Difference between control ensemble mean and observed rainfall 1931–60. Land points without observed data are shaded. Isohyets are drawn at ±0.5, 1, 2, 3, and 4 mm day^{-1}.

The control ensemble was also compared with National Centers for Environmental Prediction–National Center for Atmospheric Research reanalyses (Kalnay et al. 1996) averaged over 1979–95. The model reproduced the overall structure analyzed over TNA reasonably but there were differences in details that were often consistent with the deficiencies noted above. In particular, the dry bias in the Sahel was associated with a warm bias, and this meant the simulated lower-tropospheric heat low and African Easterly Jet (AEJ) were a few degrees farther south.

Consistent errors in different fields and reference periods indicated that these were not merely due to the somewhat arbitrary choice of reference periods. Given that the observed differences in precipitation between relatively dry and wet periods are of the order of 1 mm day^{-1} (Fig. 1), the errors in the control climate (Fig. 3b) were comparable to this signal. However, it was considered that the control climate was sufficiently similar to observations to render degradation experiments interesting, particularly if it was assumed that the sensitivity of climate to land surface processes was not greatly altered by deficiencies of the control simulation. The design and results of the degradation experiments are discussed in the following sections.

3. Degradation scenarios

The area outlined in Fig. 2 was degraded by Xue and Shukla (1993) and Xue (1997) who changed the biome

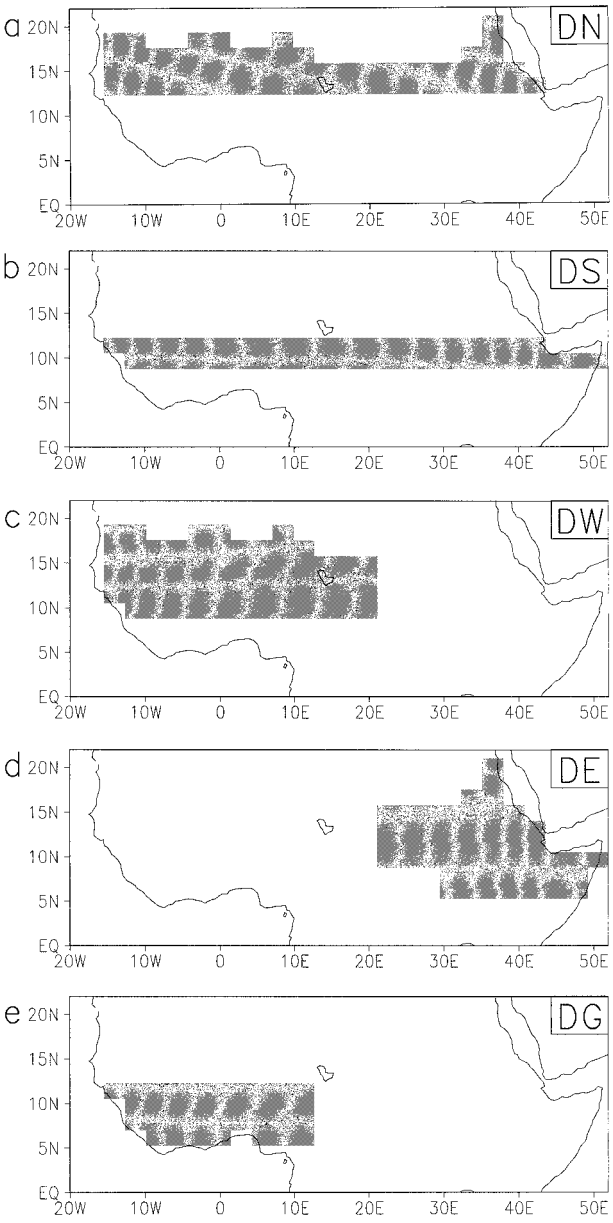

FIG. 4. Degradation scenarios for the COLA GCM. In each case the vegetation type within the shaded area was changed to type 9 to represent degradation. The vegetation types are described in Table 1: (a) DN, (b) DS, (c) DW, (d) DE, and (e) DG.

within this area to type 9 (broadleaf shrubs with bare soil) to mimic degradation. One criticism of those studies is that they may well have exaggerated the extent and severity of degradation. Since the lack of data may mean that we cannot accurately quantify historical degradation, the present work builds on the previous studies by considering less extensive degradation, which may be more realistic. Figure 4 presents the five degradation scenarios considered in the present work. In each case the biome in the area of degradation was changed to type 9. The areas seen in Figs. 4a and 4b represent northern and southern portions of the larger degraded area shown in Fig. 2, and are denoted by DN and DS, respectively. Areas DW and DE (Figs. 4c and 4d) were western and eastern parts. DE was extended to the southeast to take account of degradation in that area shown by Dregne (1983) and UNEP (1992). Area DG (Fig. 4e) was added to investigate the importance attached to deforestation in the Guinea coast area by Zheng and Eltahir (1998). Although the five areas degraded were not of equal size it was not practicable to consider equal areas without using more complicated shapes. The areas allow examination of the extent to which the location of degradation affects its impact.

The climate of TNA shows important variations with both latitude and longitude. For example, see the rainfall anomaly patterns presented by Nicholson (1980) and Nicholson and Palao (1993). Also, Thorncroft and Haile (1995) described considerable longitudinal variation of mean atmospheric structure and the nature of storms. Thus another advantage of considering smaller regions of degradation, over which the climatic regime is more nearly homogeneous, is that we can examine the extent to which differences of climate within TNA affect the sensitivity to surface characteristics.

Comparison of the degraded regions with the UNEP (1992) assessment of degradation showed that the southern part of DN was approximately the area considered as highly degraded by UNEP, suggesting that DN was the most realistic scenario. However degradation was also indicated by UNEP over a large portion of each of the other four regions. Hence although the scenarios were idealized in both extent and severity they considered an area that is thought to suffer from degradation. In view of the difficulty of prescribing historical land surface characteristics, and the rapidly increasing population of TNA, such sensitivity tests can also be viewed more generally as helping to assess the impact of possible land cover changes, both past and possibly future.

Spatial variation of the control biome type (Fig. 2) led to variation in the change of surface characteristics caused by degradation. Most scenarios involved a change from types 6 or 8 to type 9. DG included a substantial amount of type 1. In general degradation resulted in less vegetation, lower leaf area index, and a smaller surface roughness length. The soil properties of the degraded state represented a sandy soil with high hydraulic conductivity and it was assumed that the entire soil column had changed to sand. Although change to such a depth might take considerably longer than the timescale of a few decades considered here, this simplification was made as each SSiB biome includes a single soil type. The surface albedo of the degraded state was 0.30, which represented an increase of 0.10 at most points. Although Nicholson et al. (1998) suggest that the albedo could possibly have increased by as much as 0.1 since the 1950s, we again emphasize the difficulty of quantifying historical changes of the land surface at

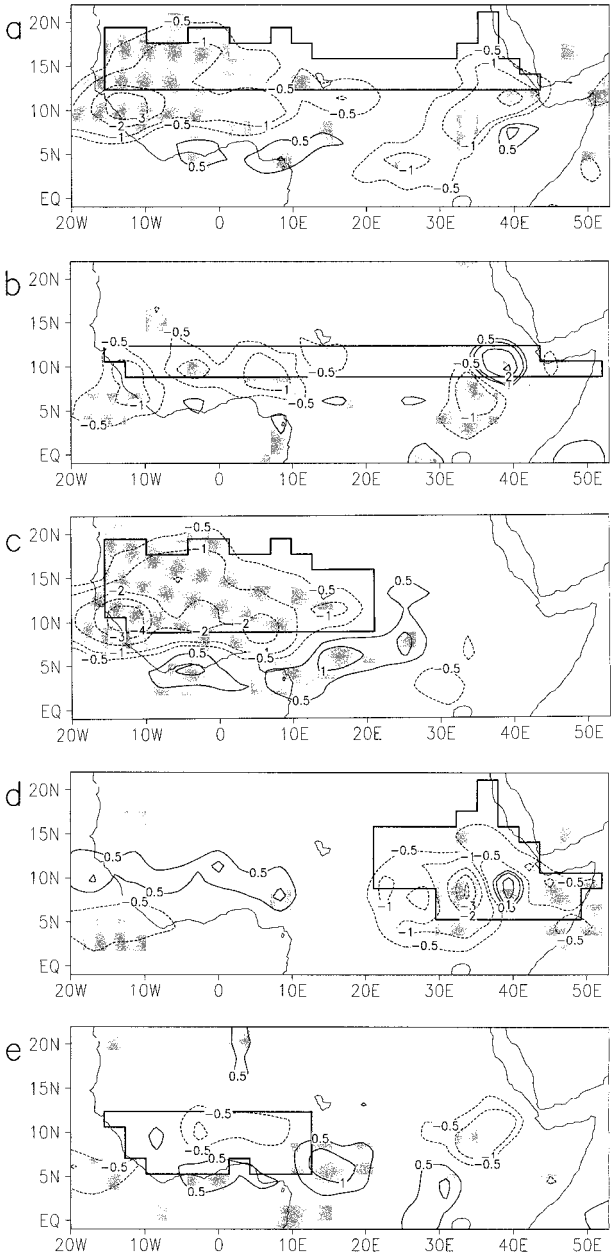

FIG. 5. JAS mean precipitation rate differences due to degradation of each of the five regions. Differences that were significant at the 95% confidence level are shaded and the degraded area in each case is enclosed by a solid line. Contours are drawn at ±0.5, 1, 2, 3, and 4 mm day^{-1}: (a) DN, (b) DS, (c) DW, (d) DE, and (e) DG.

large spatial scales and that the degradation scenarios considered here are best considered as sensitivity tests.

The degradation scenarios involved changes to several land surface parameters. Using the same version of the COLA GCM, Xue et al. (1997) found that rainfall in TNA was most sensitive to changes in surface albedo and that changes in surface roughness had less impact. On this basis it might be speculated that the albedo change may have been the most important component of the degradation scenarios considered here. However, Lean and Rowntreee (1997) noted that interaction between parameters can give surprising results and that the overall impact of land surface change needs to be assessed using changes in all relevant parameters.

TABLE 2. Differences in JAS mean precipitation rate following degradation. Values are area means over the area degraded in each case. D–C is the difference between degraded and control values. The last two columns allow comparison with the observed difference (1961–90)–(1931–60). For this, model data are only used from those points that also had observations, and both the modeled and observed change are given as a percentage to allow for bias in the control.

	Precipitation (mm day^{-1}) (all points)		Precipitation (points with obs)	
	Control	D–C	D–C (%)	Obs (%)
DN	2.1	−0.7* (−32%)	−31	−18
DS	6.8	−0.2 (−3%)	−4	−8
DW	4.0	−1.3* (−33%)	−33	−12
DE	4.8	−0.7* (−14%)	−17	−12
DG	8.1	−0.1 (−2%)	−1	−3

* The changes over the degraded area had field significance at the 99% level.

4. Impact of degradation on precipitation

The changes in JAS mean precipitation following degradation are shown in Fig. 5, while statistics averaged over the degraded area are given in Table 2. The control rainfall over TNA, and hence any change, was almost all convective in nature. The statistical significance of the change at a point was assessed by a Student's t-test. Although some of the assumptions of this test (such as equal variance in each ensemble) were not strictly satisfied, it was considered a useful estimate of approximate significance. The overall significance of the collection of point changes, that is field significance, was assessed using the binomial distribution following Livezey and Chen (1983). Table 2 includes a comparison with observed changes between 1931–60 and 1961–90 (shown in Fig. 1). These 30-yr periods were used because they are World Meteorological Organization periods for climate normals and Hulme (1992a) has described the changes in African precipitation between them. The modeled effect of degradation cannot easily be compared with observations to determine its realism since the control vegetation was not specific to a given date, the degradation scenarios were idealized and no account was taken of interdecadal SST variability. However, it is interesting to look for qualitative similarities.

After degradation of DN there was extensive reduction of precipitation in West Africa (Fig. 5a), much of which was locally significant at the 95% level. Rainfall was reduced over all the degraded region (not obvious in the figure because of the contour interval). Table 2 shows that this reduction was 32% of the control. Although the largest reductions were south of the degraded area where the control rainfall was greatest, the zonally

averaged reduction increased monotonically from 15% at 10°N to 40% at 18°N. The reductions in the east of the continent were generally not significant: both the mean and the coefficient of variation were larger there. The realism of those changes was also questionable given the poor control simulation in the area. There were small areas of modestly increased precipitation near the Guinea coast. Comparison with the observed changes (Fig. 1) indicated qualitative similarity with the contrast between the dry Sahel and wetter Guinea coast. The modeled decreases near 10°N and in the east were larger than observed, giving the larger percentage change recorded in Table 2.

Figure 5b shows that degradation of DS resulted in little change to precipitation with no field significance. Precipitation increased over the highest ground in the east but, given the poor control simulation and the complex topography of the area, the realism of this small-scale feature requires further investigation. The small meridional extent of this degraded area meant that advection from adjacent undegraded areas may well have lessened the impact of local degradation.

The pattern of rainfall changes caused by degradation of DW (Fig. 5c) was similar to that seen for DN. The difference isohyets in the north were similar in each case but the extended area of degradation in the south of DW resulted in greater change there. Over the degraded area the mean reduction was 33% of the control. Again rainfall was slightly increased south of the degraded area but there was little impact farther east, unlike the case for DN. The north–south couplet of changes was again qualitatively similar to that observed, but the large decrease simulated near 10°N and the lack of change in the east were rather different.

After degradation of DE the area of substantially reduced rainfall was small (Fig. 5d) and, as was the case for DS, degrading the highlands near 40°E resulted in a local increase. The largest changes of each sign were immediately adjacent and apparently interlinked, while elsewhere over the degraded area there were only small decreases. Small changes in West Africa were not significant.

Figure 5e shows that rainfall was not substantially altered when DG was degraded, in contrast to the results when other areas of West Africa were degraded (DN and DW). This was an area of considerable control rainfall and the changes were relatively small, so very few were statistically significant. It can be seen that rainfall decreased in the northeast of the region, while it was slightly increased nearer the coast. These opposite changes meant the area mean change was very small. The small response in this region was contrary to the findings of Zheng and Eltahir (1998) who argued that West African rainfall was particularly sensitive to coastal deforestation—a disagreement that is examined later.

These results showed that the impact of degradation varied considerably. Degradation of areas in the Sahel and West Africa resulted in the largest decreases of JAS mean precipitation. Degradation of East Africa caused less reduction, and there was negligible change when the Guinea coast was degraded. The low statistical significance of changes in East Africa was in part due to greater intra-ensemble variability. More importantly, the fractional changes in the east were also small. Xue and Shukla (1993) and Xue (1997) also found larger reductions in the west. There may be physical mechanisms, which mean that rainfall in the west is more sensitive to changes in the land surface. Cook (1994, 1997, 1999) has noted differences between West and East Africa in idealized integrations of GCMs that suggested such a sensitivity. Cook (1999) considered that an important difference was that whereas moisture converged throughout the lower troposphere in the east, there was overlying divergence in the west associated with the AEJ. The net convergence was closely tied to jet dynamics, which in turn were influenced by land surface processes.

None of the scenarios provided any evidence of a teleconnection through which changes in TNA could result in distant changes. The detection of any such signal would require more or longer runs. Even within TNA, rainfall reductions were largely restricted to the degraded areas with little effect elsewhere (except for DN). This suggested that the location of degradation was important and, if also true for the real atmosphere, that a reasonably accurate assessment of historical land cover change would be required in order to assess the impact on observed rainfall changes. However, the similarity of the response to DN and DW indicated that the sensitivity to area was not quite so extreme, and that degradation of the Sahel could have considerable impact. Given that these were essentially sensitivity tests it is perhaps sufficient to note that the simulated changes were of comparable size to those observed (Table 2), suggesting that land surface changes may have at least partly caused the observed changes of rainfall.

5. Impact of degradation of region DN

Degradation of DN is described in this section since it presented a strong signal that nonetheless included aspects common to several scenarios. Changes in seasonal means are considered first, then aspects of synoptic variability are discussed.

a. JAS mean changes

As shown in Fig. 5a, degradation of DN resulted in a substantial change of precipitation, both locally and to the south. Changes in several fields, averaged over JAS and the degraded area, are listed in Table 3. Degradation caused cloud cover to be reduced by 14%, but the effect of increased surface albedo was dominant and resulted in 20 W m^{-2} less net solar radiation at the surface (S_n). Surface temperature (T_s) increased in the west, where rainfall reductions were large, but decreased

TABLE 3. JAS mean differences due to degradation of DN. Values are means over the degraded area. D–C is the difference between degraded and control values. Here θ_e in the boundary layer is for the lowest level for which data were analyzed—on average this was within 50 hPa of the surface.

	Control	D–C
Cloud cover	0.42	−0.06 (−14%)
S_n (W m^{-2})	241	−20** (−8%)
L_n (W m^{-2})	−90	−9 (+10%)
R_n (W m^{-2})	151	−29** (−19%)
H (W m^{-2})	102	−14** (−14%)
LE (W m^{-2})	50	−15* (−30%)
T_s (K)	307.1	+0.2
Boundary layer θ_e (K)	343.4	−2.7
P (mm day^{-1})	2.1	−0.7* (−32%)
E (mm day^{-1})	1.7	−0.5* (−30%)
MC (mm day^{-1})	0.4	−0.2 (−50%)

* Significant at the 90% confidence level.
** Significant at the 95% confidence level.

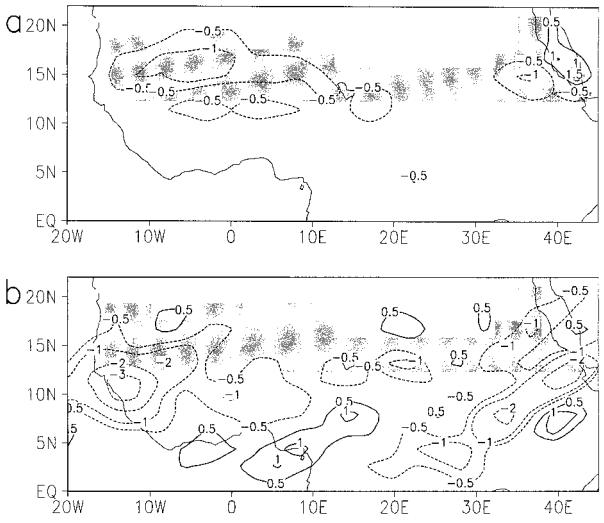

FIG. 6. JAS mean changes in components of the water budget due to degradation of region DN. The degraded area is shaded. Contours are drawn at ±0.5, 1, 2, and 3 mm day^{-1}: (a) evaporation and (b) vertically integrated moisture flux convergence.

farther east, so there was a small increase in the mean. This meant that the area mean 9 W m^{-2} reduction of net longwave radiation at the surface (L_n) was almost entirely due to a smaller downwelling flux from less cloud cover and a drier lower troposphere, with little change in the area mean upward flux. Thus the changes in the short- and longwave parts of the spectrum were in the same sense and the net radiation (R_n) was 29 W m^{-2} (19%) less after degradation.

The reduction of R_n was met by almost equal contributions from H and LE. Over the degraded area, rainfall, R_n and surface roughness were reduced, all of which would tend to lower LE. Evaporation in the control was already partly limited by water availability and hence the large reduction of R_n also led to reduced H over most of the degraded area.

Despite being warmer after degradation, the boundary layer was also substantially drier and the equivalent potential temperature (θ_e, calculated after Bolton 1980) decreased by over 2 K. This suggests that, once initiated, moist convection was less vigorous after degradation. Because of feedbacks it is difficult to distinguish cause and effect—lower θ_e could result in less rainfall, but equally, less rainfall could alter the surface fluxes so as to lower θ_e.

The moisture budget for an atmospheric column can be written as $P = E + \text{MC}$, where P is the rate of precipitation, E is the rate of evaporation from the surface, MC is the vertically integrated moisture flux convergence and the budget is evaluated over a season so that changes in storage are generally negligible. Figure 6 shows the changes of E and MC following degradation and should be compared with the rainfall change shown in Fig. 5a. Over the degraded area the reduction of P was largely balanced by reduced E with a smaller contribution from reduced MC, consistent with the dominance of P and E in the control moisture balance (see Table 3). South of the degraded area there was relatively little change of E; here the clearer sky that accompanied lower P meant slightly increased R_n which, together with the fact that rainfall was still relatively abundant, tended to maintain E. With little change of E the substantial reduction of P south of DN was associated with reduced MC. The similarity of E and P changes over the degraded area should not be interpreted solely in terms of local recycling of water vapor, that is that less E meant less water was available for rainfall. Rainfall in any area generally consists of both water that evaporated locally and water that was advected in. The efficiency with which the water content of the atmosphere is converted to rainfall depends partly on local thermodynamic conditions. Local evaporation can influence the efficiency through its effect on boundary layer moisture. Hence evaporation has a double role, both providing moisture and influencing thermodynamic profiles. The recycling rate and the precipitation efficiency can be estimated from model data (e.g., Brubaker et al. 1993; Gong and Eltahir 1996), but this was not possible in the present study due to the limited model diagnostics saved. Previous studies have estimated that approximately 25%–40% of rainfall in West Africa is derived from recycled rainfall (Brubaker et al. 1993; Gong and Eltahir 1996). Since the reduction of P was in fact larger than that of E we conclude that it is unlikely that this was solely due to the recycling mechanism. It is likely that both reduced recycling and lower precipitation efficiency contributed to the rainfall reduction, at least qualitatively as described by Schär et al. (1999) in a European setting. Without further data we cannot test this hypothesis.

As regards the atmospheric circulation, many of the effects of degradation appeared as a weakening of the control circulation, coupled with a slight southward displacement. Figure 7 shows the vertical velocity in pres-

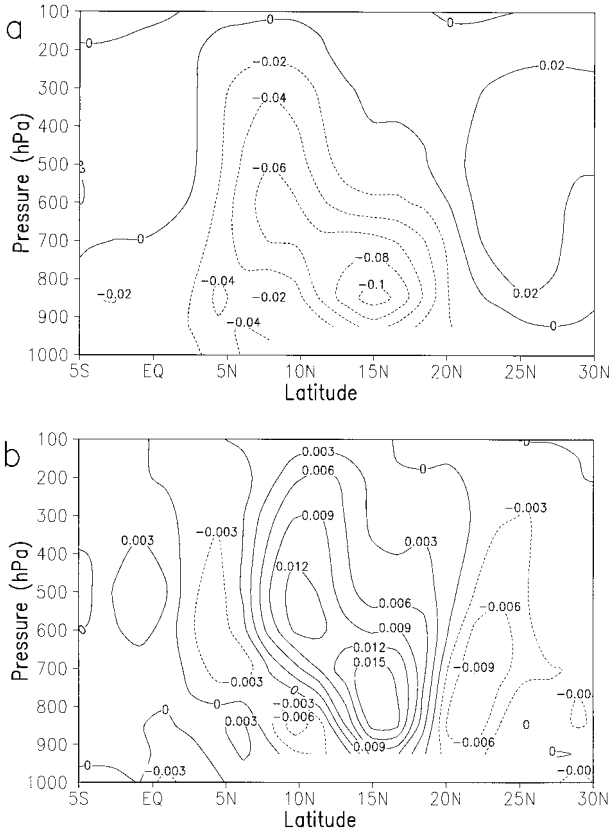

FIG. 7. The effects of degradation of region DN on JAS mean ω (Pa s^{-1}) averaged over 15°W–40°E: (a) control and (b) change after degradation. The degraded area was approximately 12°–18°N. Points below the surface are left blank.

sure coordinates (ω) averaged between 15°W and 40°E over TNA for the control and the difference following degradation. In the control (Fig. 7a), relatively shallow ascent occurred over the heat trough near 15°N with ascent throughout the depth of the troposphere in the main rain belt near 9°N. Following degradation there was relative descent over most of DN (Fig. 7b), consistent with relative divergence at low levels. Areas of relative descent were associated with reduced parameterized heating. Although the contributions of component parameterizations were not saved, it was likely that the reduced heating at midlevels was dominated by reduced convective heating, as found by Xue (1997). South of the degraded area, near 10°N, H increased following degradation and there was relative ascent at low levels, but this was replaced by relative descent aloft. Increased shallow ascent would tend to remove moisture from the boundary layer and make deep convection less likely (Sud and Molod 1988). Increased ascent in the midtroposphere near 5°N was associated with increased rainfall, as seen in Fig. 5a.

To a first approximation, the changes of meridional wind following degradation were consistent with slight weakening of the Hadley circulation, with weaker flow in both low levels and the upper troposphere. Intraensemble variability in the horizontal winds was high and few changes were statistically significant. No significant change was found in the strength of the AEJ, indeed there was little change in the zonal wind at that height. This contrasts with the observed tendency for dry years in the Sahel to be associated with a stronger AEJ (e.g., Newell and Kidson 1984), and with the stronger AEJ in response to modeled degradation reported by Xue (1997).

In summary, reduced R_n and lower availability of moisture from the degraded surface led to reduced evaporation and a warmer, drier boundary layer. Consistent with this there was less moist convection and weaker large-scale ascent. Reduced low-level convergence of mass and moisture fed back to strengthen the signal of less moist convection. The new balance between the land surface, cumulus convection, and the large-scale flow was such that there was a weaker overturning circulation in TNA and less rainfall. This changed regional circulation meant that rainfall was also reduced in areas outside the degradation area, and drier conditions in those areas would in turn contribute to the weaker overall circulation. Although the details of the interaction of components of the GCM was complicated, the modeled climate of a large area of TNA was sensitive to land surface conditions in region DN.

b. Synoptic variability in region DN

In a GCM study, Polcher (1995) found that the response of tropical convection to land surface changes could be interpreted in terms of changes in the characteristics of daily rainfall events. Thus the study of variability on these shorter timescales may add to our understanding of the mechanisms by which degradation affects seasonal precipitation. This section describes some simple statistics of the variability and how these changed with degradation.

An important aspect of synoptic variability in West Africa are African Easterly Waves (AEWs). These have a mean wavelength in the range 2000–4000 km, period 3–5 days and are often associated with squall lines and substantial precipitation (e.g., Burpee 1972; Reed et al. 1977; Duvel 1990). As regards the present work, Clark (1999) showed that spectra of the meridional wind at 850 hPa (ν_{850}) from the control ensemble compared favorably with these observational results. Figure 8a shows the contribution to the area mean rainfall made by events of different sizes. The daily rainfall (p) at each point within the degraded area was sorted into three classes, holding values $p \leq 1$, $1 < p \leq 5$, and $p > 5$ mm, respectively. In the control ensemble, the largest class of events produced most of the rainfall, despite being only 14% of the total number (Fig. 8b). Hovmoeller plots and other analyses showed that these largest events were associated with AEW. In general it appeared that the control ensemble showed synoptic var-

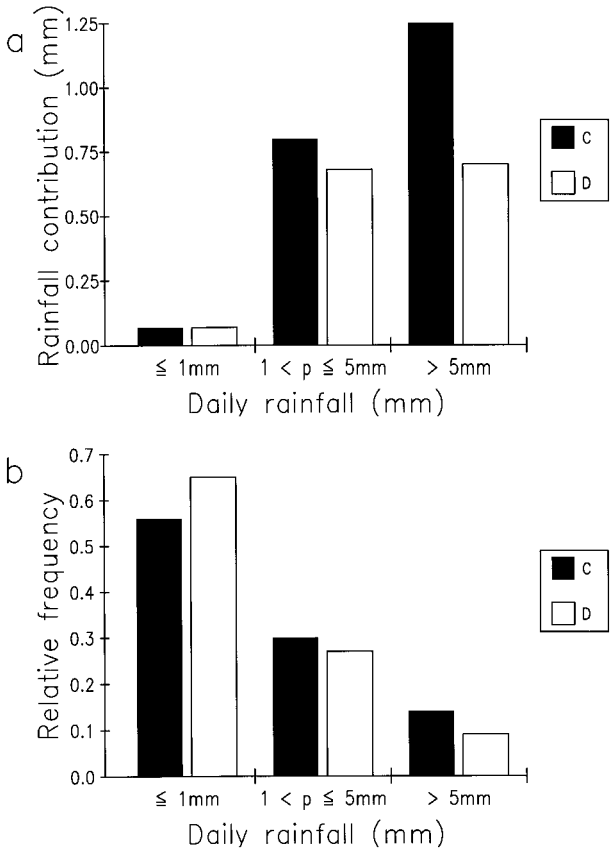

FIG. 8. Statistics of daily rainfall over region DN for the control (C) and degradation (D) ensembles. The daily rainfall data were separated into three classes according to size. (a) The contribution to the JAS area mean rainfall made by gridpoint daily totals in each class. (b) The relative frequency of gridpoint daily totals in each class.

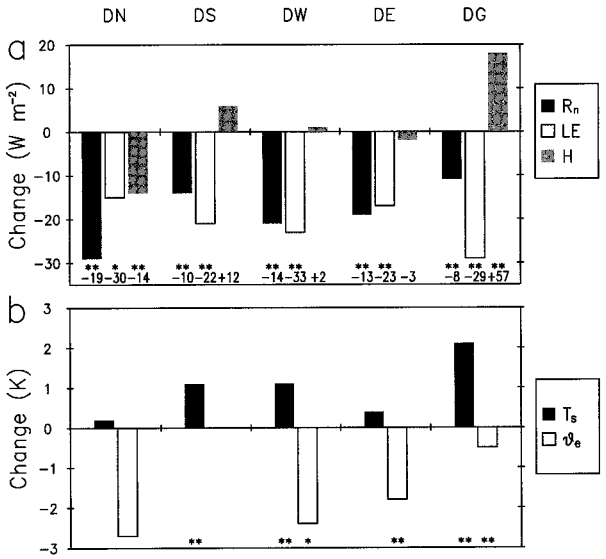

FIG. 9. JAS mean differences caused by degradation of the five regions studied. Values are means over the area degraded in each case. Differences that were significant at the 90% and 95% confidence levels are marked * and **, respectively, at the foot of each graph, and percentage differences are also listed there (not for temperatures), (a) Net radiation, latent heat flux and sensible heat flux (W m^{-2}) and (b) surface temperature and boundary layer θ_e (K).

iability in West Africa which was at least broadly similar to that observed.

After degradation of DN, spectra of ν_{850} showed no clear change in the amplitude, peak period or spatial distribution of the variance. Similarly, no significant change was found in the number of waves seen in Hovmoeller plots of ν_{850}. Of the rainfall reduction following degradation, 82% was due to changes in the wettest class, principally because there were fewer events. Days of little or no rainfall increased in frequency, while the numbers in both wetter classes decreased (Fig. 8b). Similar conclusions held when only points west of 10°E (the area of well-developed AEWs) were analyzed. Since the occurrence of waves was unchanged (shown by ν_{850}) we conclude that the mean rainfall produced by each wave was less after degradation. Thus, although AEWs continued to propagate across West Africa after degradation, the local hydrology had changed so that large rainfall events were less likely.

The present analysis agrees with the result of the GCM runs of Xue and Shukla (1993), that degradation gave an approximately unchanged number of disturbances but the mean event rainfall was lowered. It also agrees with the finding of Polcher (1995) from tropical deforestation experiments that the main effect is fewer large rain events. Rain gauge data indicate that low rainfall in southern Niger over recent decades was due to fewer events while the mean event size had not changed (Le Barbé and Lebel 1997). Most of the rainfall in the Sahel comes from mesoscale systems (Lebel et al. 1997) that are too small to be explicitly represented in the GCM. Deficiencies in the parameterized representation of the effects of such systems may explain some of the disagreement with the present work. Further work is required to investigate the physical mechanisms relating synoptic disturbances and rainfall, and their sensitivity to land surface processes.

6. Impact of degradation: Comparison of all regions

Having considered degradation of DN in some detail in the previous section, we now compare the effect of degradation of each of the five regions considered, largely focusing on JAS mean quantities and the surface energy balance.

Figure 9 shows changes in JAS means averaged over the area degraded in each case—thus each average refers to a different area. There were a number of similarities between regions. All regions had reduced cloud cover following degradation (not shown, and the reduction was sometimes small), but in all cases the effect of increased surface albedo was greater and led to reduced

S_n. This was an important factor in causing lower R_n in all regions (Fig. 9a). Smaller reductions of S_n in the wetter southern areas (not shown) were consistent with the removal of deeper clouds with higher albedo, as suggested by Xue (1997). This was partly why there was relatively little reduction of R_n over DG, the wettest area considered. The LE was also reduced in all regions, often by more than the reduction of R_n, indicating the importance of greater surface resistance to evaporation (due to reduced availability of moisture and less vegetation cover). The H showed changes of both sign and was generally thought of as responding to the residual left after changes of R_n and LE had been accounted for. Thus in DN the large reduction of R_n was not matched by reduced LE since this was limited by water availability and vegetation cover, and so H decreased. But in DG the smaller reduction of R_n and greater reduction of LE (allowed by the removal of dense vegetation) resulted in increased H.

The time and area mean thermodynamic profiles all showed small changes with degradation, consistent with warmer, drier boundary layers. Surface temperature increased in every case (Fig. 9b), with the large increases in areas DS, DE, and DG explained by the large reductions of LE there. However, boundary layer θ_e decreased in most cases, reflecting lower humidity. Substantially reduced θ_e was found in the three regions where rainfall was greatly reduced.

Figure 10 shows the components of the JAS mean water balance for each region. Values are shown for the change caused by degradation and the control case. Despite the similarity of the percentage changes of E (all were reduced by 22%–33%, Fig. 10a) there was a wide range in the response of P (from -32% to -2%), corresponding to variation of the change in MC. The similarity of the E changes was partly due to similarity of the imposed degradation, while the different P changes reflected differences in the surface–atmosphere interaction: in some areas the changed surface had a dramatic effect on the atmosphere, in others the effect was less. A large reduction of P occurred where both E and MC decreased (DW and DN, in the latter MC was small), a smaller reduction occurred where MC was little changed (DE), and P was effectively unchanged where MC was increased (DS and DG). To better understand the results we would need to understand the response of MC, but this is complicated by feedbacks between different processes. Increased MC accompanied increased H in DS and DG, and in other cases this correlation existed in certain parts of the degraded area. However, given that large increases of MC would be expected to be associated with rainfall and a wet surface from which H would be small, the details of the relationship between H and MC are unclear.

We can speculate that an important characteristic of DN was the dominance of E over MC in the control (Fig. 10b). Qualitatively this suggested a regime in which local evaporation exerted considerable influence

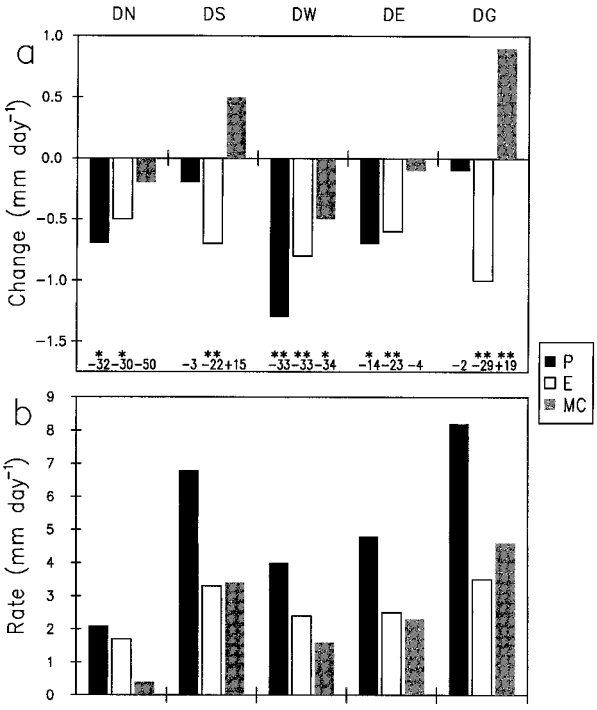

FIG. 10. Components of the JAS mean water balance (mm day^{-1}) for each of the five regions studied. Values are means over the area degraded in each case. (a) Changes after degradation. Differences that were significant at the 90% and 95% confidence levels are marked * and **, respectively, at the foot of each graph, and percentage differences are also listed there. (b) Control values.

on atmospheric moisture, so that changes of evaporation could cause substantial changes in thermodynamic profiles. Certainly the large reduction of E caused by the removal of vegetation was accompanied by a dramatic decrease of rainfall. The opposite case was illustrated by region DG, over which MC was equivalent to 56% of the control rainfall. In that case, the reduction of E following degradation had less impact because of compensating MC. Although the increase of MC was substantial, it was less than 20% of the control value for that area. A similar increase in DN would have represented a change of over 200% and was thus much less likely. Region DE represented an intermediate case with approximately equal E and MC in the control. Degradation there caused a small decrease of MC but this was only a small fraction of the control and hence the reduction of P was relatively small. Qualitatively, Fig. 10 shows a pattern in which increasing importance of E in the control water balance meant increasing sensitivity to degradation, but further investigation is needed to fully understand the mechanisms at work.

Degradation had the least impact on precipitation in DG. The degradation was most severe in this region, so that, in the simplest argument, a large impact on rainfall might be anticipated. However, R_n was reduced by a relatively small amount consistent with a southern position, as discussed above. The removal of relatively

lush vegetation resulted in a large decrease in LE which, together with relatively little change to R_n, meant that there was a large increase in surface temperature. According to the linear model of Eltahir and Bras (1993) this was indeed consistent with increased convergence and convective instability, which would tend to keep rainfall plentiful. However, a more realistic analysis must consider the effect on moist thermodynamics, as noted by Eltahir (1996) and others. Boundary layer humidity was only slightly reduced, despite a large reduction of evaporation, due to increased moisture advection from the south and west where the ocean represented a plentiful supply of moisture. Further, the higher temperature of boundary layer air substantially offset the effect of slight drying and θ_e in the boundary layer was only slightly reduced. Again this was consistent with the small effect on rainfall. However, as the small change of boundary layer θ_e could also be interpreted as a *result* of the small change of rainfall, rather than a cause, this argument cannot be fully closed. In many respects the changes in DG were not very different from those elsewhere and it is not clear why the impact on rainfall was so small. It may be that DG was simply more extreme—the degradation was more severe, the temperature rise was larger, and moisture advection from the adjacent ocean was large. It is clear that the final response of the GCM is the net result of many effects.

7. Discussion and conclusions

This paper has described the use of seasonal integrations of the COLA GCM to investigate the impact of idealized land surface degradation on the climate of tropical north Africa. This study advances the work of Xue and Shukla (1993) and Xue (1997) by considering five regions within TNA. The impact of degradation was often substantial, with less vegetation and higher albedo leading to less evaporation and rainfall, as in the previous studies. However, the impact varied considerably between regions, with degradation in the northern Sahel and West Africa having the greatest impact on rainfall. In these regions both evaporation and moisture convergence were reduced. Farther east, there was a less dramatic impact on rainfall, consistent with little change in the moisture convergence. To the south, in an area including the Guinea coast, there was negligible change in rainfall, and increased moisture convergence compensated for the large decrease of evaporation.

The only similar work is that of Zheng and Eltahir (1998, hereafter ZE98) who used a zonally symmetric model with a simple representation of the land surface to simulate degradation of different latitudes. In the present work DN, DS, DW, and DG represented degradation of different latitudes in West Africa (see Fig. 4; the greater zonal extent of DN was not thought to have had a large effect). ZE98 found that degradation of various bands between 10° and 20°N resulted in locally reduced rainfall but increased rainfall south of the degraded area. In the present work, the results for DN and DW broadly support this finding. However, whereas ZE98 found that deforestation in the south resulted in a greatly weakened monsoon flow and reduced rainfall across much of TNA, degradation of DG in the COLA GCM had minimal impact on rainfall. Both studies found reduced evaporation but the changes of MC were very different, and the large reduction of θ_e found by ZE98 was not reproduced in the COLA GCM. Possible reasons for the differences between the studies include differences in the nature of the prescribed degradation and the numerical models. In particular we note that the land surface parameterization used in the COLA GCM is relatively sophisticated and so, hopefully, more realistic. Also, the response of the COLA GCM included stronger westerly flow and moisture advection across the western boundary of the degraded region, a response that was not possible in the two-dimensional case. The extent to which rainfall is sensitive to the structure of synoptic disturbances ultimately determines whether a two-dimensional representation is sufficient. This question remains to be answered.

The possibility that the initial condition, particularly of soil moisture, exerted a strong control throughout the 4-month period of each integration and therefore biased the results cannot be discounted without comparison with longer integrations. However, we note that Xue (1997) reported that such a comparison in a very similar case showed that the impact of model spinup on most quantities, including evaporation and rainfall, was minimal.

Although the seasonal mean statistics examined here summarize the effects of degradation, they do not tell us *why* each area responded as it did. A target for future work should be to understand the mechanisms causing the differences between regions. One potentially useful approach is the diagnostic analysis of the low-level vorticity balance to investigate the processes linking the surface and atmosphere, as described by Cook (1997). Important differences may also lie in the details of the structure of a typical rainfall event and in the development of the boundary layer between events, details that cannot be analyzed via seasonal mean diagnostics. Examples of insight provided by analysis of such details using daily or more frequent data are given by Polcher (1995) and Schär et al. (1999).

This study emphasizes the importance of the interaction between the atmosphere and the land surface in determining climate. It also supports the possibility of a positive feedback, first proposed by Charney (1975), in which anthropogenic degradation leads to less rainfall, which in turn may make further degradation more likely. In particular this study supports the idea that land degradation in the Sahel, such as may have occurred this century, leads to a widespread reduction of rainfall that is qualitatively similar to changes observed in recent decades. However, these remain sensitivity studies,

with the extent and severity of degradation idealized. The absence of observations of land cover over sufficient time-and space scales with which to describe the historical land surface may prevent firm conclusions being reached as to why rainfall was persistently low in recent decades. For the recent past and future, more realistic experiments may be possible with land surface characteristics derived from remote sensing, and these should use contemporaneous SST observations so model results can be directly compared with observed rainfall. Finally, further realism may be added by the use of interactive vegetation models in which the growth of vegetation depends upon the simulated climate and in which anthropogenic effects might be included as a disturbance. Recent work in this direction is that of Wang and Eltahir (2000).

Acknowledgments. The authors would like to thank C. Taylor, A. Culf, and J. Gash at CEH, Wallingford, Oxfordshire, United Kingdom, and two anonymous reviewers for comments that helped to improve the manuscript. This work was partly supported by NSF Grant EAR9706403. The assistance of M. Fennessy with running the GCM is appreciated. Rainfall data ''gu23wld0098.dat'' (Version 1.0) was constructed and supplied by Dr. Mike Hulme at the Climatic Research Unit, University of East Anglia, Norwich, United Kingdom, supported by the U.K. Department of the Environment, Transport and the Regions (Contract EPG 1/1/48).

REFERENCES

Anthes, R. A., 1977: A cumulus parameterization scheme utilizing a one-dimensional cloud model. *Mon. Wea. Rev.*, **105,** 270–286.

Barkstrom, B. R., 1984: The Earth Radiation Budget Experiment (ERBE). *Bull. Amer. Meteor. Soc.*, **65,** 1170–1185.

Bolton, D., 1980: The computation of equivalent potential temperature. *Mon. Wea. Rev.*, **108,** 1046–1053.

Bottomley, M., C. K. Folland, J. Hsiung, R. E. Newell, and D. E. Parker, 1990: *Global Ocean Surface Temperature Atlas 'GOSTA.'* UKMO/MIT. 20 pp. and 313 plates.

Brubaker, K. L., D. Entekhabi, and P. S. Eagleson, 1993: Estimation of continental precipitation recycling. *J. Climate,* **6,** 1077–1089.

Burpee, R. W., 1972: The origin and structure of easterly waves in the lower troposphere of North Africa. *J. Atmos. Sci.*, **29,** 77–90.

Charney, J. G., 1975: Dynamics of deserts and drought in the Sahel. *Quart. J. Roy. Meteor. Soc.*, **101,** 193–202.

——, W. J. Quirk, S.-H. Chow, and J. Kornfield, 1977: A comparative study of the effects of albedo change on drought in semi-arid regions. *J. Atmos. Sci.*, **34,** 1366–1385.

Clark, C. A., and R. W. Arritt, 1995: Numerical simulations of the effect of soil moisture and vegetation cover on the development of deep convection. *J. Appl. Meteor.*, **34,** 2029–2045.

Clark, D. B., 1999: Modelling the impact of land surface degradation on the climate of tropical North Africa. Ph.D. thesis, University of Reading, 264 pp. [Available from University of Reading, Whiteknights, Reading RG6 6AH, United Kingdom.]

Cook, K. H., 1994: Mechanisms by which surface drying perturbs tropical precipitation fields. *J. Climate,* **7,** 400–413.

——, 1997: Large-scale atmospheric dynamics and Sahelian precipitation. *J. Climate,* **10,** 1137–1152.

——, 1999: Generation of the African easterly jet and its role in determining West African precipitation. *J. Climate,* **12,** 1165–1184.

De Ridder, K., 1997: Land surface processes and the potential for convective precipitation. *J. Geophys. Res.*, **102,** 30 085–30 090.

Diedhiou, A., and J. F. Mahfouf, 1996: Comparative influence of land and sea surfaces on the Sahelian drought: A numerical study. *Ann. Geophys.–Atmos. Hydros. Space Sci.*, **14,** 115–130.

Dregne, H. E., 1983: *Desertification of Arid Lands.* Hardwood Academic Publications, 242 pp.

——, M. Kassas, and B. Rozanov, 1991: A new assessment of the world status of desertification. *Desert. Control Bull.,* **20,** 6–18.

Duvel, J. P., 1990: Convection over tropical Africa and the Atlantic Ocean during northern summer. Part II: Modulation by easterly waves. *Mon. Wea. Rev.*, **118,** 1855–1868.

Eltahir, E. B., 1996: Role of vegetation in sustaining large-scale atmospheric circulations in the tropics. *J. Geophys. Res.*, **101,** 4255–4268.

——, and R. L. Bras, 1993: On the response of the tropical atmosphere to large-scale deforestation. *Quart. J. Roy. Meteor. Soc.*, **119,** 779–793.

Fennessy, M. J., and Coauthors; 1994: The simulated Indian monsoon: A GCM sensitivity study. *J. Climate,* **7,** 33–43.

Fischer, G., and G. K. Heilig, 1997: Population momentum and the demand on land and water resources. *Philos. Trans. Roy. Soc. London B,* **352,** 869–889.

Gong, C. L., and E. A. B Eltahir, 1996: Sources of moisture for rainfall in West Africa. *Water Resour. Res.,* **32,** 3115–3121.

Harshvardhan, R. Davies, D. A. Randall, and T. G. Corsetti, 1987: A fast radiation parameterization for atmospheric circulation models. *J. Geophys. Res.*, **92,** 1009–1016.

Hou, Y.-T., 1990: Cloud–radiation–dynamics interaction. Ph.D. thesis, University of Maryland, College Park, MD, 209 pp.

Hulme, M., 1992a: Rainfall changes in Africa: 1931–1960 to 1961–1990. *Int. J. Climatol.*, **12,** 685–699.

——, 1992b: A 1951–80 global land precipitation climatology for the evaluation of general circulation models. *Climate Dyn.,* **7,** 57–72.

Janicot, S., V. Moron, and B. Fontaine, 1996: Sahel droughts and ENSO dynamics. *Geophys. Res. Lett.*, **23,** 515–518.

Kalnay, E., and Coauthors, 1996: The NCEP/NCAR 40-Year Reanalysis Project. *Bull. Amer. Meteor. Soc.,* **77,** 437–471.

Kinter, J. L., III, J. Shukla, L. Marx, and E. K. Schneider, 1988: A simulation of the winter and summer circulations with the NMC global spectral model. *J. Atmos. Sci.,* **45,** 2486–2522.

Kuchler, A. W., 1984: World map of natural vegetation. *Goode's World Atlas,* 16th ed., E. B. Espenshade Jr., Ed., Rand Mcnally, 16–17.

Kuo, H. L., 1965: On formation and intensification of tropical cyclones through latent heat release by cumulus convection. *J. Atmos. Sci.,* **22,** 40–63.

Lamb, P. J., and R. A. Peppler, 1991: West Africa. *Teleconnections Linking Worldwide Climate Anomalies,* M. Glantz, R. W. Kats, and N. Nicholls, Eds., Cambridge University Press, 121–189.

Lare, A. R., and S. E. Nicholson, 1994: Contrasting conditions of surface water balance in wet years and dry years as a possible land surface–atmosphere feedback mechanism in the West African Sahel. *J. Climate,* **7,** 653–668.

Le Barbé, L., and T. Lebel, 1997: Rainfall climatology of the HAPEX-Sahel region during the years 1950–1990. *J. Hydrol.,* **189,** 43–73.

Lean, J., and P. R. Rowntree, 1997: Understanding the sensitivity of a GCM simulation of Amazonian deforestation to the specification of vegetation and soil characteristics. *J. Climate,* **10,** 1216–1235.

Lebel, T., J. D. Taupin, and N. D'Amato, 1997: Rainfall monitoring during HAPEX-Sahel. 1. General rainfall conditions and climatology. *J Hydrol.,* **188–189,** 74–96.

Livezey, R. E., and W. Y. Chen, 1983: Statistical field significance

and its determination by Monte Carlo techniques. *Mon. Wea. Rev.*, **111,** 46–59.

Mellor, G. L., and T. Yamada, 1982: Development of a turbulence closure-model for geophysical fluid problems. *Rev. Geophys.*, **20,** 851–875.

Mintz, Y., and G. K. Walker, 1993: Global fields of soil moisture and land surface evapotranspiration derived from observed precipitation and surface air temperature. *J. Appl. Meteor.*, **32,** 1305–1334.

Newell, R. E., and J. W. Kidson, 1984: African mean wind changes between Sahelian wet and dry periods. *J. Climatol.*, **4,** 27–33.

Nicholson, S. E., 1980: The nature of rainfall fluctuations in subtropical West Africa. *Mon. Wea. Rev.*, **108,** 473–487.

——, 1993: An overview of African rainfall fluctuations of the last decade. *J. Climate*, **6,** 1463–1466.

——, and I. M. Palao, 1993: A re-evaluation of rainfall variability in the Sahel. Part I. Characteristics of rainfall fluctuations. *Int. J. Climatol.*, **13,** 371–389.

——, C. J. Tucker, and M. B. Ba, 1998: Desertification, drought, and surface vegetation: An example from the West African Sahel. *Bull. Amer. Meteor. Soc.*, **79,** 815–829.

Polcher, J., 1995: Sensitivity of tropical convection to land surface processes. *J. Atmos. Sci.*, **52,** 3143–3161.

Reed, R. J., D. C. Norquist, and E. E. Recker, 1977: The structure and properties of African wave disturbances as observed during Phase III of GATE. *Mon. Wea. Rev.*, **105,** 317–333.

Rowell, D. P., C. K. Folland, K. Maskell, and M. N. Ward, 1995: Variability of summer rainfall over tropical north Africa (1906–92): Observations and modelling. *Quart. J. Roy. Meteor. Soc.*, **121,** 669–704.

Sato, N., D. A. Randall, P. J. Sellers, E. K. Schneider, J. Shukla, J. L. Kinter III, Y.-T. Hou, and E. Albertazzi, 1989: Implementing the Simple Biosphere Model (SiB) in a general circulation model: Methodologies and results. NASA Contractor Rep. 185509, 76 pp.

Schär, C., D. Luthi, U. Beyerle, and E. Heise, 1999: The soil–precipitation feedback: A process study with a regional climate model. *J. Climate*, **12,** 722–741.

Schiffer, R. A., and W. B. Rossow, 1983: The International Satellite Cloud Climatology Project (ISCCP): The first project of the World Climate Research Programme. *Bull. Amer. Meteor. Soc.*, **64,** 779–784.

Segal, M., R. W. Arritt, C. Clark, R. Rabin, and J. Brown, 1995: Scaling evaluation of the effect of surface characteristics on potential for deep convection over uniform terrain. *Mon. Wea. Rev.*, **123,** 383–400.

Slingo, J. M., 1987: The development and verification of a cloud prediction scheme for the ECMWF model. *Quart. J. Roy. Meteor. Soc.*, **113,** 899–927.

Sud, Y., and A. Molod, 1988: The roles of dry convection, cloud-radiation feedback processes, and the influence of recent improvements in the parameterization of convection in the GLA GCM. *Mon. Wea. Rev.*, **116,** 2366–2387.

——, and W. M. Lau, 1996: Variability of summer rainfall over tropical north Africa (1906–92)—Observations and modelling—comment. *Quart. J. Roy. Meteor. Soc.*, **122,** 1001–1006.

Thorncroft, C. D., and M. Haile, 1995: The mean dynamic and thermodynamic fields for July 1989 over tropical North Africa and their relationship to convective storm activity. *Mon. Wea. Rev.*, **123,** 3016–3031.

Tiedtke, M., 1983: The sensitivity of the time mean large scale flow to cumulus convection in the ECMWF model. *Proc. Workshop on Convection in Large Scale Numerical Models*, Reading, United Kingdom, ECMWF, 297–316.

Tucker, C. J., H. E. Dregne, and W. W. Newcomb, 1991: Expansion and contraction of the Sahara desert from 1980 to 1990. *Science*, **253,** 299–301.

UNEP, 1992: *World Atlas of Desertification.* Edward Arnold, 69 pp.

Wang, G., and E. A. B. Elathir, 2000: Biosphere–atmosphere interactions over West Africa. II: Multiple climate equilibria. *Quart. J. Roy. Meteor. Soc.*, **126,** 1261–1280.

Xue, Y., 1997: Biosphere feedback on regional climate in tropical North Africa. *Quart. J. Roy. Meteor. Soc.*, **123,** 1483–1515.

——, and J. Shukla, 1993: The influence of land surface properties on Sahel climate. Part I: Desertification. *J. Climate*, **6,** 2232–2245.

——, P. J. Sellers, J. L. Kinter III, and J. Shukla, 1991: A simplified biosphere model for global climate studies. *J. Climate*, **4,** 345–364.

——, J. A. Elbers, F. J. Zeng, and A. J. Dolman, 1997: GCM parameterization for Sahelian land surface processes. *HAPEX-Sahel West Central Supersite: Methods, Measurements and Selected Results*, P. Kabat, S. Prince, and L. Prihodko, Eds., The Winand Staring Centre for Integrated Land, Soil and Water Research, Rep. 130. HM/07.97, 289–297.

Zheng, X. Y., and E. A. B. Eltahir, 1998: The role of vegetation in the dynamics of West African monsoons. *J. Climate*, **11,** 2078–2096.